INDIAN JOURNAL OF SCIENCE AND TECHNOLOGY

RESEARCH ARTICLE

Joining of Al-Alloy Tubes by Carbon Steel Tubes using MPW Technique

K Gnanamurugan[1]*, R Varahamoorthi[2], C Sundarraj[3]

1 Research Scholar, Department of Manufacturing Engineering, Faculty of Engineering and Technology, Annamalai University, Annamalai Nagar, 608 002, Tamil Nadu, India
2 Professor, Department of Manufacturing Engineering, Faculty of Engineering and Technology, Annamalai University, Annamalai Nagar, 608 002, Tamil Nadu, India
3 Professor/Principal, AVC College of Engineering, Mannampandal, Mayiladuthurai, Tamil Nadu, India

OPEN ACCESS

Received: 23-01-2024

Accepted: 22-05-2024

Published: 17-06-2024

Citation: Gnanamurugan K, Varahamoorthi R, Sundarraj C (2024) Joining of Al-Alloy Tubes by Carbon Steel Tubes using MPW Technique. Indian Journal of Science and Technology 17(24): 2538-2546. https://doi.org/10.17485/IJST/v17i24.177

* **Corresponding author**.

gnanamurugank08@gmail.com

Funding: None

Competing Interests: None

Published By Indian Society for Education and Environment (iSee)

ISSN
Print: 0974-6846
Electronic: 0974-5645

Abstract

Background/ Objectives: Joining aluminum alloys with low carbon steel (DC01) through fusion welding is a challenging task due to the occurrence of solidification defects like porosity, alloy segregation, and hot cracking. However, these issues can be addressed by employing solid-state welding techniques like explosive welding and MPW (magnetic pulse welding). MPW is a cost-effective and high-speed solid state welding method that involves creating joints in an overlap configuration. **Methods:** The MPW technique was employed to join dissimilar aluminum alloy AL 7075T6 hollow tube and DC01 steel rod in this study. A central composite design model was created to analyze the relationship between key MPW process parameters, including stand-off distance (SoD), overlap length, and discharge energy, and the bonding strength of the joints. Experimental setups were established and correlate with tensile-shear fracture load and interface hardness of the joints with the MPW process parameters. **Findings:** It is understood that the maximum TSFL of 2.404 kN was obtained under the welding condition of 23kJ discharge energy, 2.25 mm Stand-off distance, 8.5 mm overlap length, which is the optimum MP welding state for AA 7075 T6 with DC01 and confirmed by RSM. In addition, the cultivated connection can be aptly leveraged to anticipate the TSFL of MPW joints with a 95% confidence level. **Novelty:** The parametric mathematic samples were developed for forecasting TSFL of joints. The MPW parameters were optimized to enhance TSFL of joints. Aluminium alloys with low carbon steel joints were developed using MPW for cars and ships applications without fusion welding defects.

Keywords: Magnetic Pulse Welding; Dissimilar Joint; (RSM) Response Surface Methodology; Tensile Shear-Fracture Load

1 Introduction

Lightweight construction and energy efficiency are having a strong impact on the new product development (NPD). The recent engineering system should concentrate on

developing the ground-breaking lightweight design and, at the same time, the global environmental and economic advantages of the entire product lifecycle (PLC). Particularly for the automotive industry the subject of lightweight design represents one of the most major innovation drivers and technology trends [1]. The utilization of the dual metallic welding structure, comprising steel and aluminium, has emerged as the favored option for achieving lightweight designs in industrial manufacturing. This approach necessitates the connection between steel and aluminium, which has been extensively researched by scholars from various countries [2]. The joining of different metals has garnered significant attention, particularly in the context of steel and aluminium, as it is crucial for fabricating complex structures used in automobiles and ships [3]. To establish a metallurgical behavior and heating is required; however, in the case of dissimilar- joints (Al/Steel), a higher heat input frequently results in the form of brittle and intermetallic phases. These phases have the potential to compromise the mechanical behavior of the bond [4].

MPW is a solid- state welding method that has grown significant consideration in the welding community. It offers the capability to join both similar and dissimilar materials within microseconds, without the requirement of contact between the work piece and welding consumables. The MPW process functions in a manner akin to explosive welding, where the dynamic effects produced by the collision of the joining components at high impact velocities are crucial for successful bonding. When arranged in a cylindrical configuration, the components intended for joining are placed concentrically within a coil, resulting in the formation of an acceleration gap. The electromagnetic pulse welding (MPW) technique utilizes a brief pulse duration of less than 100 μs to propel the flyer work piece towards a target part. The application of electric current to the coil results in the generation of a concentrated magnetic field surrounding the coil. This magnetic field, in turn, induces currents within the conductive outer work piece. These induced currents, known as eddy currents, act in opposition to the magnetic field produced by the coil. As a consequence, a repulsive force is created, leading to the development of high pressure on the outer component. This pressure surpasses the yield strength of the material, and it is the result of the interaction between the two magnetic fields. This pressure propels the outer component through the standoff gap due to the repulsion, culminating in a concentrated pressure at the point of collision. Due to the collision's subsonic velocity, pressure is exerted on the nearby surfaces, resulting in the abrasion of a thin layer of metal. The angled collision produces significant shear stress at the interface, causing the elimination of oxides and impurities from both surfaces [5]. MPW process driven by two major units. The first one is an electrical pulse generator (EPG), second unit is the workstation, is to convert the given electrical pulse into a pulse magnetic field [6]. Two main configurations are used with the MPW process: sheet lap joint and tubular lap joint [7].

Among these methods, response surface methodology (RSM) stands out as a commonly employed technique to analyze the interaction effect between input parameters. By utilizing RSM, researchers can effectively study and optimize the input process parameters to achieve the desired mechanical properties in welded joints. In this particular investigation, Aluminium alloy and carbon steel were joined using the magnetic pulse welding technique, and the process parameters of discharge energy (kJ), standoff distance (mm), and overlap length (mm) were optimized using RSM to achieve the maximum shear load.

2 Experimental Procedure

2.1 Important parameters

The investigation was conducted on a magnetic pulse welded machine, specifically designed for steel coil (EN-8), with an energy capacity of 100 kJ. This machine is manufactured by Magpulse Technologies Pvt Ltd. The study aimed to define the main aspects that affect the tensile shear fracture load of the magnetic pulse welded joints. The independent parameters considered in the experiment were the applied discharge energy (KJ), stand-off distance (mm), and overlap length (mm). Through the analysis, it was found that these parameters exerted a substantial influence on the fracture load of the joints [8].

2.2 Working parameters

The trial runs of the experiment were conducted by utilizing hollow AL 7075T6 with thickness of 2 mm and a DC01 low carbon steel pipe. The objective was to determine the feasible working limits of magnetic pulse welding parameters. Various parameters were employed during the test trails. The inspection of the welded surface and weld quality was carried out to ascertain the working limits of weld parameters. As a result, the subsequent observation was made: when the discharge energy was extended to 23KJ, the joint was separated. Furthermore, for discharge energy exceeding 27 kV, significant deformation was observed on the weld joints. If the discharge energy falls below 23KJ, the joint will separate, while a discharge energy exceeding 27KJ will result in higher deformation observed on the welded joints. A stand-off distance less than 2.25 mm will cause the joint to separate, whereas a stand-off distance greater than 2.5 mm will lead to deformation of the flyer aluminum. In cases where the overlap length is less than 7.05 mm, the joint will separate, but if the overlap length exceeds 8.5 mm, separation of the weld

will be observed [9].

2.3 Design Matrix Development

Major selection of possible parameter range was determined based on the given condition to ensure defect-free welding of the hollow AL 7075T6 alloy. The factors range considered is presented in Table 1 **,** while Table 2 displays the 20 sets of coded conditions used to create the design of matrix. To facilitate the processing of test data, the lower and upper ranges of the factors were implied as +1.682 and -1.682, correspondingly. The methodology for designing this matrix is explained elsewhere [10].

3 Results and Discussions

The experiment's solution heat treated AL 7075T6 aluminum alloy of 2 mm wall thickness the length of 35 mm, diameter- 66mm fixed and seam welded DC01 carbon steel of 63 mm wall thickness the length of 30 mm**,** lab joint consignation was prepared to fabricate MPW joints and also SD is playing a manger change on steel rod diameter 60.5, 61, 61.5, 62, 62.5 respectively. The initial joint consignation was obtained by securing the tubes in position using High Density Polyethylene (HDPE). The direction weld was normal to the aluminium positioned direction. Single pulse was used to fabricate the joints.

The fabricated joints were sliced from the MPW joint by Electron Discharge Marching (EDM) to attain required shape size. Each specimen three strips (samples) prepared. Two specimens were used to assess the fracture load in tensile shear. The test was conducted using an electromechanical controlled universal testing machine, and the average values of the two results were obtained.

Table 1. Important MPW parameters

No.	Parameter	Unit	-1.68	-1	0	1	1.68
1	Discharge energy	kV	21	23	25	27	29
2	Stand-off-distance	mm	1.75	2	2.25	2.5	2.75
3	Overlap length	mm	6.50	7.00	7.50	8.00	8.50

RSM encompasses a collection of mathematical and statistical tools utilized to examine scenarios where numerous variables have an impact on a specific response of interest. The primary aim of RSM is to optimize this response by thoroughly analyzing the relationships between the variables and the desired outcome. By employing RSM, researchers can effectively navigate complex problems and identify the most favorable conditions for achieving the desired response. In the case of the joint, the response function for the tensile shear fracture load (TSFL) is dependent on discharge energy (V), stand-off distance (D), and overlap length (L), and can be stated as:

$$TSFL = f(E, D, L) \tag{1}$$

Various experimental design techniques can be utilized to estimate the regression coefficients. For this study, central composite design was employed to accurately model the second order response surface. The coefficients were determined using the Design Expert statistical software package through central composite design. Subsequently, the significant coefficients were identified and used to establish the final relationship. The experimental relationship to predict tensile shear fracture load of magnetic pulse welded aluminium tube with carbon steel tubular joints is given as:

Table 2. Experimental results and Design matrix

Ex. No	Implied Values			Definite Values			TSFL
	E	D	L	E	D	L	
1	-1	**-1**	**-1**	13	1	7	1.73
2	+1	-1	-1	15	1	7	1.5
3	-1	+1	-1	13	2	7	2.4
4	+1	+1	-1	15	2	7	2.32
5	-1	-1	+1	13	1	8	1.5
6	+1	-1	+1	15	1	8	1.29
7	-1	+1	+1	13	2	8	1.29

Continued on next page

Table 2 continued

8	+1	+1	+1	15	2	8	1.25
9	-1.50	0	0	12.3182	1.5	7.5	2.33
10	+1.50	0	0	15.6818	1.5	7.5	2.07
11	0	-1.50	0	14	0.659104	7.5	1.14
12	0	+1.50	0	14	2.3409	7.5	1.67
13	0	0	-1.50	14	1.5	6.6591	2.01
14	0	0	+1.50	14	1.5	8.3409	0.9
15	0	0	0	14	1.5	7.5	2.1

TSFL = {-65.14 + 0.035 E + 8.88 D +1 6.85 L + 0.09 ED + 5×10-3EL - 0.85 DL - 9.96×10-3 (E) 2 –1.14 (D) 2 - 1.08636 (L) ^{2}} kN.

3.1 Testing adequacy of developed model

The developed model capability was assessed through application of the analysis of variance technique (ANOVA). By comparing the designed Fratio value of the developed relation with the typical Fratio value (from the F-table) at a preferred confidence range (95%), it can be determined whether the developed model is satisfactory inside the given confidence limit. The ANOVA test outcomes and a comparative discussion of various processes are provided in Tables 3 and 4. It can be concluded that the developed model is acceptable with a 95% confidence level.

Table 3. Comparative studies of different process and techniques

S. no	Different Process	Observations	Reference
1	The welding procedure parameters for joining dissimilar austenitic and duplex stainless steels can be modified to enhance resistance spot welding.	A maximum TSFL of 1.501 kN was obtained under the welding condition	(11)
2	The mechanical properties of friction stir spot weld bonds were analyzed in terms of tensile-shear behavior.	Compared to tests, the maximum joint tensile shear fracture load error was 10.8%.	(12)
3	The optimization of FSW parameters for enhancing the strength of lap joints in AA2014-T6 aluminum alloy is investigated in this study.	The rotational speed of 900 rpm resulted in achieving a maximum TSFL of 1.276 kN.	(13)

Table 4. ANOVA test results

Source	Sum of squares	df	Mean square	F value	P Value (Prob>F)	
Model	3.79	9	0.48	7149.3	< 0.0001	Major
E-E	0.068	1	0.069	1155.06	0.0002	
D-D	0.3326	1	0.38	5650.59	< 0.0001	
L-L	1.47	1	1.47	25041.2	< 0.0001	
E-D	0.0128	1	0.016	217.44	0.017	
V-L	4.00E-05	1	5.00E-05	7.64	0.877	
D-L	0.3785	1	0.36	6429	< 0.0001	
E2	1.43E-03	1	1.43E-03	301.08	0.4157	
D2	0.8473	1	1.18	14393.1	< 0.0001	
L2	0.7282	1	1.06	12370.9	< 0.0001	
Residual	0.02	10	1.98E-03			
Lack of fit	0.012	5	2.31E-03	0.2179	0.94	Not major
Pure error	0.0005	5	0.0001			
Cor total		3.79		19		
Standard Deviation	0.0077		R-Squared	0.99		
Mean	1.8		Adj R-Squared	0.99		
C.V %	0.4271		Pred R-Squared	0.99		
Press	0.1		Adeq Precision	275.8062		

The significance of the relationship is indicated by the model F-value of 7149.30, which suggests that there is a strong relationship. The probability of this large ”model F-value” occurring due to noise is only 0.01%. Model terms such as E, D, L, ED, EL, DL, E2, D2, and L2 are considered significant, as their ”prob>F” values are less than 0.0500. On the other hand, relationship terms with values greater than 0.1000 are deemed not significant. The lack of fit F-value of 0.2190 suggests that the lack of fit is not significant compared to the pure error. The degree of determination, denoted as ”r2”, serves as a measure to evaluate the proximity of predicted values to the actual experimental values. In the context of the relationship established and outlined in Table 5, the ”r2” value signifies a strong correlation between the predicted and experimental values. Notably, the ”Pred. R-squared” value of 0.99 aligns well with the ”adj R-squared” value of 0.99, indicating a consistent level of accuracy. Lastly, the ”Adeq precision” metric quantifies the signal-to-noise ratio, providing insights into the reliability of the data.

4 Optimization of MPW Parameters

Table 5 llustrates the objective, lower and upper limits, as well as the significance of each response and factor within the optimization criterion. Meanwhile, Table 6 presents a compilation of MPW parameters achieved through optimization criteria. The optimization tool employed to determine the optimal values of the process variables was the response surface methodology (RSM).

The experimental relationship established in the preceding section was formulated based on the coded values assigned. The optimization process involved working with these coded values before translating them into their corresponding actual values. The optimization of the process variables was carried out using the Design Expert statistical software package. Under the optimum

Table 5. Criteria for numerical optimization

Name	Goal	Lower Limit	Upper Limit	Lower Weight	Upper Weight	Importance
A:Discharge energy	is in range	23	15	1	1	3
B:Stand-off-distance	is in range	2	2	1	1	3
C:Overlap length	is in range	8.5	8	1	1	3
TSFL	maximize	0.9	2.4	1	1	3

Table 6. Optimal welding solutions

Number	Discharge energy (kJ)	Stand-off-distance (mm)	Overlap length (mm)	TSFL	Desirability	
1	**23.087**	**2**	**8.5**	**2.404**	0.981	**Selected**
2	13.067	1.933	7.009	2.407	0.978	
3	13.057	1.889	7.015	2.413	0.974	
4	13.029	1.970	7.015	2.402	0.970	
5	13.057	1.810	7.052	2.411	0.961	
6	13.105	1.755	7.003	2.403	0.953	

Conditions, a maximum tensile shear fracture load of 2.404 KN. Figure 1 illustrates the strong relationship between the experimental and predicted values of the TSFL. Response surfaces were The contour response surfaces clearly indicate the optimal response point, which is determined by taking two parameters on the ’X’ and ’Y’ axes and the response on the ’Z’ axis. This empirical relationship has been developed to analyze and understand the relationship between these variables. By visualizing the contour response surfaces, researchers can easily identify the point that yields the most desirable outcome.

In Figures 2 and 3, it can be observed that the apex of the contour response surface exhibits the optimum tensile shear strength of MP welded AL 7075T6 to DC01. The contour plots display a distinctive circular mound shape, which suggests the possible independence of factors in relation to the region of optimal factor settings. By utilizing software for response surface analysis and generating contour plots, the shape of the surface can be characterized, allowing for the accurate identification of the optimum point. Circular contour patterns signify the autonomy of factor influences, whereas elliptical contours may indicate factor relationships. Figures 2 and 3 illustrate the best response for MP welded AL 7075T6 to DC01 tube.

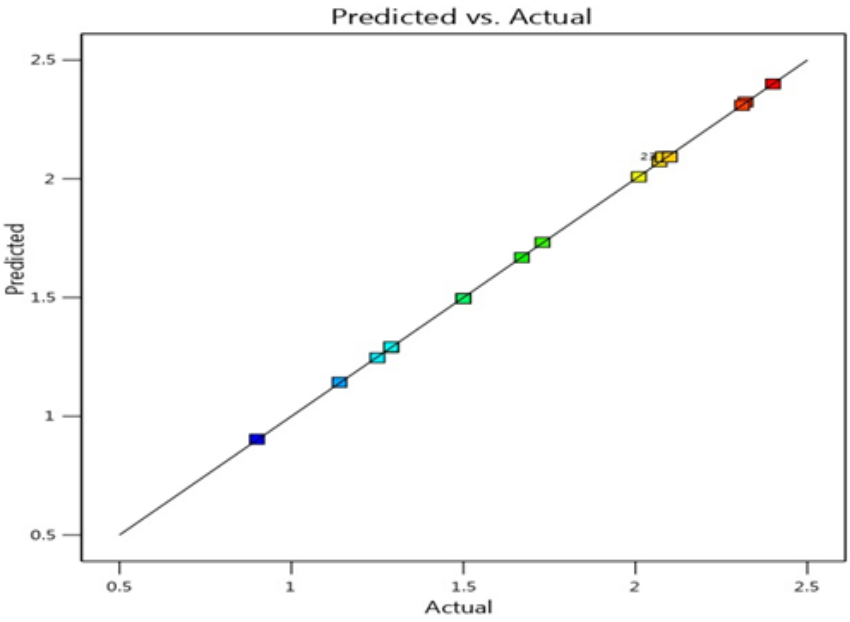

Fig 1. Correlation graph of TSFL

5 Response Graphs and Contour Plots Analysis

The optimization technique of RSM resulted in the creation of 3D surface graphs and contour plots, which were generated by a model with one parameter fixed at the middle level while the other two parameters varied. The 3D response surface graph and contour plot illustrated that as the stand-off distance increased at a constant discharge energy, the TSFL initially rose to a peak value before decreasing. Standoff distance 0.5 mm to 2 mm and increase in discharge energy 23 kJ to 27 kJ, at the time of collision, kinetic energy of the outer tube (AL 7075 T6) is lower due to lower standoff distance due to that impact velocity is reduced and tensile shear fracture load is decreases.

At standoff distance 1 mm to 2 mm at a given discharge energy the maximum TSFL (2.404 kN) is achieved. In the case the kinetic energy of the outer tube (AL 7075T6) is increases at critical discharge energy converted to heat by massive plastic deformation of the metals.

Standoff distance 2 mm to 2.5 mm at a given discharge energy, the TSFL is decreases. In the case of increasing stand-off distance, it is directly proportional to the angle of collision and kinetic energy of the flyer (aluminium). The plastically deformed metal with increasing kinetic energy increasing the shearing effect and decreasing the stability of the flyer. Its lead to decreases the TSFL. Figure 3 shows 3D response surface graph and contour plot, with increasing overlap length at a given discharge energy, the TSFL fist increases to a maximum value and afterwards shown a decrease with increase in overlap length.

Overlap length 6.5 mm to 7.5 mm and decrease the TSFL (shown in Figure 4**c**)), because of the flyer is at the open end and is situated in the middle of the field shaper or coil (where the magnetic flux density is high), this area is exposed to the extreme magnetic pressure, concentrated on the center of the coil and also the collision velocity is higher.

Figure 3**(c and f)** shows the 3D response surface graph and contour plot, with increasing standoff distance at a given overlap length, the TSFL fist increases to a maximum value and afterwards shown a decrease. Figure 4 shows the effect of welding parameters on TSFL. The TSFL was decreased with increasing. Discharge energy from 13kV to 15kV. The same trend was observed in the working distance. The TSFL fist increases to a maximum value and afterwards shown a decrease with stand-off-distance is increases.

Validation:

Five tests using the optimized process parameter values were carried out in order to verify and test the projected TSFL of RSM. The fact that the maximum mistake is 4% indicates how predictive the current optimization techniques are.

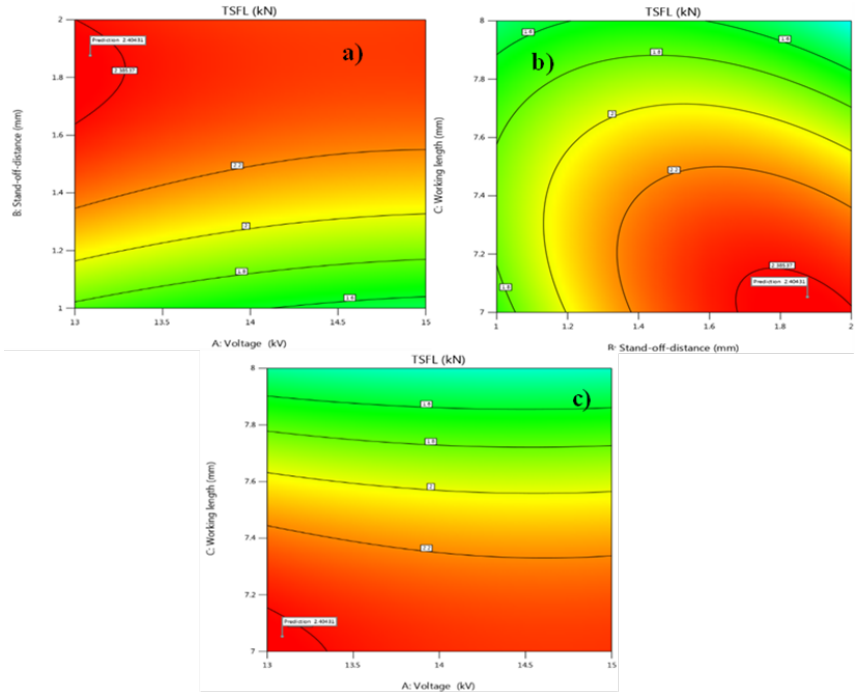

Fig 2. Contour graphs of TSFL a) Discharge energy vs Stand-off-distance, b) Stand-off-distance vs. overlap length and c) Discharge energy vs overlap length

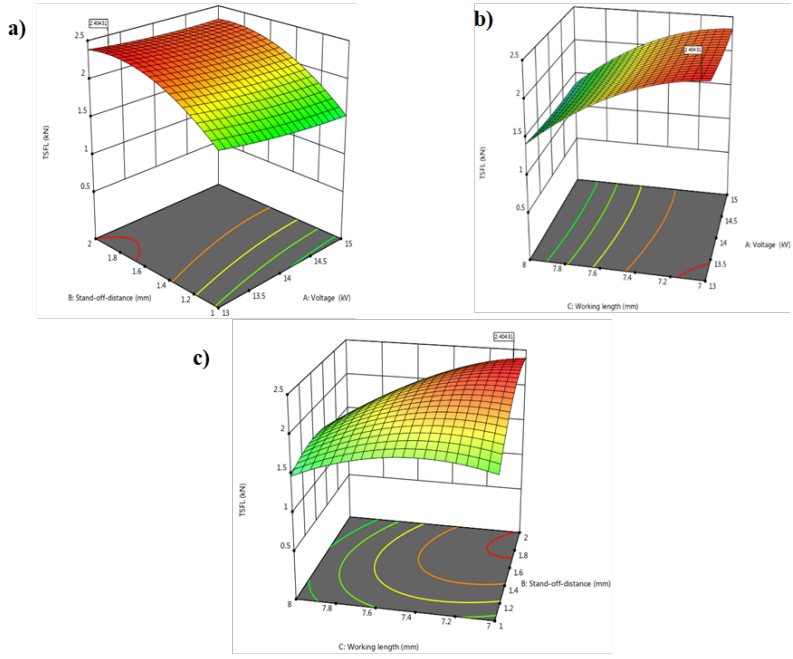

Fig 3. 3D response graphs of TSFL a) Discharge energy vs Stand-off-distance, b) Discharge energy vs overlap length and c) Stand-off-distance vs overlap length

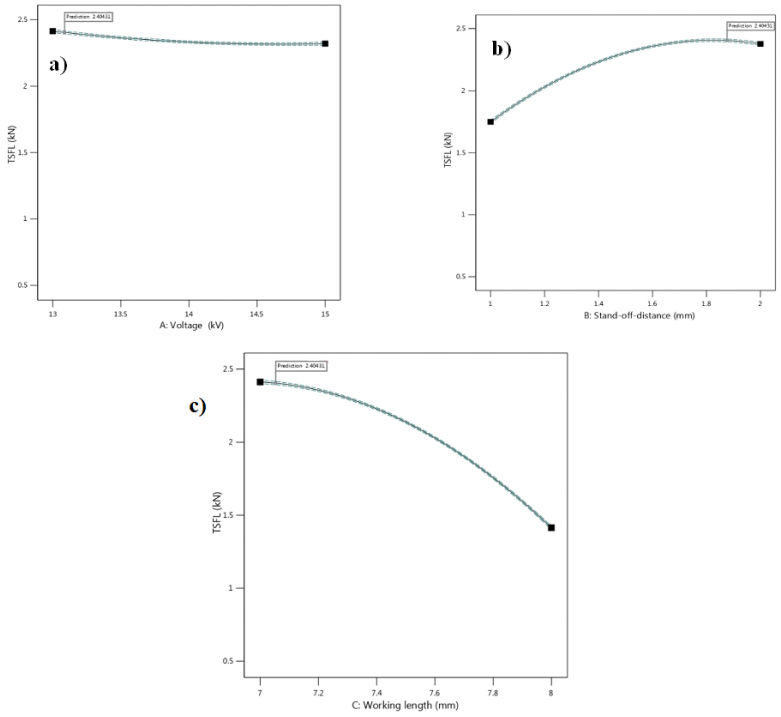

Fig 4. Direct effect of welding parameters on TSFL

6 Conclusions

1. RSM was employed to establish an experimental correlation for estimating the TSFL of AL 7075T6 Al alloy tube joined with DC01 carbon steel tube through magnetic pulse welding. This developed relationship offers an effective means of predicting the TSFL of magnetic pulse welded joints with a 94% assurance level.
2. A maximum TSFL of 2.404 kN was found under the weld condition of 23kJ discharge energy, 2.25 mm Stand-off distance, 8.5 mm overlap length, which is the optimum MP welding condition for AA 7075 T6 with DC01 and established by RSM.
3. Overlap length has the greatest effect on TSFL, followed by applied discharge energy, and stand-off distance.
4. Combining aluminum alloy tubes with carbon steel tubes poses difficulties as a result of the varying metallurgical and physical characteristics of the two materials. The fusion welding process, like arc welding, between steel and aluminum may result in the development of fragile intermetallic phases, rendering the connections inadequate for numerous uses.

References

1) Han Y, Chen J, Ma H, Zhao X, Wu C, Gao J. Numerical simulation of arc and droplet behaviors in TIG-MIG hybrid welding. Materials. *Materials* . 2020;13(20). Available from: https://doi.org/10.3390/ma13204520.
2) Carvalho GHSFL, Galvão I, Mendes R, Leal RM, Loureiro A. Microstructure and mechanical behaviour of aluminium-carbon steel and aluminium-stainless steel clads produced with an aluminium interlayer. *Materials Characterization*. 2019;155. Available from: https://doi.org/10.1016/j.matchar.2019.109819.
3) Pereira D, Oliveira JP, Santos TG, Miranda RM, Lourenço F, Gumpinger J, et al. Aluminium to Carbon Fibre Reinforced Polymer tubes joints produced by magnetic pulse welding. *Composite Structures*. 2019;230. Available from: https://doi.org/10.1016/j.compstruct.2019.111512.
4) Cui J, Li Y, Liu Q, Zhang X, Xu Z, Li G. Joining of tubular carbon fiber-reinforced plastic/aluminum by magnetic pulse welding. *Journal of Materials Processing Technology*. 2019;264:273–282. Available from: https://doi.org/10.1016/j.jmatprotec.2018.09.018.
5) Verma S, Kumar V, Kumar R, Sidhu RS. Exploring the application domain of friction stir welding in aluminum and other alloys. *Materials Today: Proceedings*. 2022;50(Part 5):1032–1042. Available from: https://doi.org/10.1016/j.matpr.2021.07.449.
6) Kutiová K, Měsíček J, Krzikalla D. Experimental examination of adhesive bonded carbon Fibre tube to aluminum alloy AW 7075. *InMaterials Science Forum*. 2020;994:125–132. Available from: https://doi.org/10.4028/www.scientific.net/MSF.994.125.
7) Jiang B, Chen Q, Yang J. Advances in joining technology of carbon fiber-reinforced thermoplastic composite materials and aluminum alloys. *The International Journal of Advanced Manufacturing Technology*. 2020;110:2631–2649. Available from: https://doi.org/10.1007/s00170-020-06021-2.

8) Selvaraj R, Shanmugam K, Selvaraj P, Balasubramanian V. Optimization of process parameters of rotary friction welding of low alloy steel tubes using response surface methodology. *Forces in Mechanics*. 2023;10:1–20. Available from: https://doi.org/10.1016/j.finmec.2023.100175.
9) Kumar S, Singh R. Optimization of process parameters of metal inert gas welding with preheating on AISI 1018 mild steel using grey based Taguchi method. *Measurement*. 2019;148. Available from: https://doi.org/10.1016/j.measurement.2019.106924.
10) Sundaraselvan S, Senthilkumar N, Balamurugan T, Kaviarasu C, Sathishkumar GB, Rajesh M. Optimization of friction welding process parameters for Joining Al6082 and mild steel using RSM. *Materials Today: Proceedings*. 2023;74(Part 1):91–96. Available from: https://doi.org/10.1016/j.matpr.2022.11.401.
11) Krishnan V, Ayyasamy E, Paramasivam V. Influence of resistance spot welding process parameters on dissimilar austenitic and duplex stainless steel welded joints. *Proceedings of the Institution of Mechanical Engineers*. 2021;235(1):12–23. Available from: https://doi.org/10.1177/0954408920933528.
12) Guishen Y, Xin C, Zitao W. Effect of adhesive ductility and joint configuration on the tensile-shear behaviors of friction stir spot weld bonding joints. *The Journal of Adhesion*. 2022;98(11):1663–1686. Available from: https://doi.org/10.1080/00218464.2021.1932484.
13) Rajendran C, Srinivasan K, Balasubramanian V, Balaji H, Selvaraj P. Identifying combination of friction stir welding parameters to maximize strength of lap joints of AA2014-T6 aluminium alloy. *Australian Journal of Mechanical Engineering*. 2019;17(2):64–75. Available from: https://doi.org/10.1080/14484846.2017.1304843.